



# SIMULATION OF DELAMINATION PROPAGATION IN COMPOSITES UNDER HIGH-CYCLE FATIGUE USING COHESIVE-ZONE MODELS

A. Turon\*, J. Costa\*, P. P. Camanho\*\*, J.A. Mayugo \*

\* AMADE, Universitat de Girona, Spain, \*\* DEMEGI, Universidade de Porto, Portugal

**Keywords:** *Delamination, fatigue, cohesive zone models*

## Abstract

*A damage model is proposed for the simulation of delamination growth under high-cycle fatigue. The basis for the formulation is an interfacial degradation law that links fracture mechanics and damage mechanics to relate the evolution of the damage variable,  $d$ , with the crack growth rate  $da/dN$ . The damage state is a function of the loading conditions as well as the experimentally-determined crack growth rates for the material. The formulation ensures that the experimental results can be reproduced by the analysis without the need of additional adjustment parameters.*

## 1 Introduction

High-cycle fatigue is a common cause of failure of aerospace structures. In laminated composite materials, the fatigue process involves several damage mechanisms that result in the degradation of the structure. One of the most important fatigue damage mechanisms is interlaminar damage (delamination).

There are two basic approaches for the analysis of delamination under fatigue: Linear Elastic Fracture Mechanics, which relates the fatigue crack growth rate to the energy release rate and mode-ratio, and damage Mechanics, where the concept of a cohesive zone is used to establish damage evolution as a function of the number of cycles.

Under general cyclic loading, the total damage is the sum of the damage caused by static or quasi-static loads and the damage that results from the cyclic loads. For high-cycle fatigue, the damage evolution that results from cyclic loads is usually

formulated as a function of the number of cycles and strains (or displacement jumps) [1–3]. A damage evolution law expressed in terms of the number of cycles is established a priori by adjusting several parameters through a trial-and-error calibration of the analysis [1–3].

In this paper, an approach is proposed whereby the evolution of damage derives from a Fracture Mechanics description of the fatigue crack growth rate. The approach is formulated using the cohesive zone model concept. A constitutive damage model previously developed by the authors for static or quasi-static loads [4-5] is enhanced to incorporate a damage evolution law for high-cycle fatigue. In the present model for fatigue damage, the evolution of the damage variable associated with cyclic loading is derived from a Fracture Mechanics description of the fatigue crack growth rate. Therefore, the proposed model links Fracture Mechanics to Damage Mechanics.

The model relates damage accumulation to the number of load cycles while taking into account the loading conditions (load ratio,  $R$ , energy release rate,  $G$ , and fracture mode-ratio). When used in a structural analysis, the model can simulate the dependence of the crack growth rate on these parameters. In addition to the Paris Law crack growth regime, the model also exhibits a threshold value for no growth as well as quasi-static tearing.

The new fatigue damage model is implemented as a user-written element in ABAQUS [6] based on the cohesive finite element previously developed by the authors [5].

## 2 Simulation using cohesive elements

### 2.1 Cohesive zone model approach

The CZM approach [7-9] is one of the most commonly used tools to simulate quasi-brittle fracture. The CZM approach represents a damage zone that develops near the tip of a crack and assumes that all inelastic material response can be lumped to a surface ahead of the crack tip.

Cohesive damage zone models relate tractions,  $\tau$ , to displacement jumps,  $\Delta$ , at the interfaces where crack propagation occurs. Damage initiation is related to the interfacial strength of the material,  $\tau^o$ . When the energy dissipated is equal to the fracture toughness of the material,  $G_c$ , the traction is reduced to zero and new crack surfaces are formed.

### 2.2 Numerical representation of the CZM

The constitutive law used is a bilinear relation between the tractions and the displacement jumps [4,5]. The bilinear cohesive law uses an initial linear elastic response before damage initiation, as shown in Figure 1. This linear elastic part is defined using a penalty stiffness parameter,  $K$ , that ensures a stiff connection between the surfaces before crack propagation. The interfacial strength and the penalty stiffness define an onset displacement jump,  $\Delta^o$ , related to the initiation of damage.

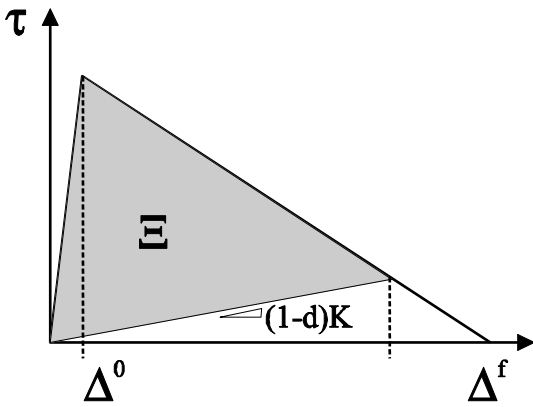


Fig. 1. Bilinear constitutive law used for quasi-static loads.

#### 2.2.1 Kinematics and constitutive model for quasi-static loading

The displacement jump across the interface  $[[u_i]]$ , is obtained from the displacements of the points located on the top and bottom sides of the interface,  $u_i^+$  and  $u_i^-$ , respectively:

$$[[u_i]] = u_i^+ - u_i^- \quad (1)$$

where  $u_i^\pm$  are the displacements with respect to a fixed Cartesian coordinate system. A co-rotational formulation is used to express the components of the displacement jumps with respect to the deformed interface. The coordinates  $\bar{x}_i$  of the deformed interface are [10]:

$$\bar{x}_i = X_i + \frac{1}{2}(u_i^+ + u_i^-) \quad (2)$$

where  $X_i$  are the coordinates of the undeformed interface.

The components of the displacement jump vector in the local coordinate system on the deformed interface,  $\Delta_m$ , are expressed in terms of the displacement field in global coordinates:

$$\Delta_m = \Theta_{mi} [[u_i]] \quad (3)$$

where  $\Theta_{mi}$  is the rotation tensor, defined in [4,5].

The constitutive operator of the interface,  $D_{ji}$ , relates the element tractions,  $\tau_j$ , to the displacement jumps,  $\Delta_i$ :

$$\tau_j = D_{ji} \Delta_i \quad (4)$$

The constitutive model must compute accurately the energy dissipated by fracture. Under mixed-mode loading, a criterion established in terms of an interaction between components of the energy release rates associated with each fracture mode is used to predict crack propagation. The formulation

of the damage model previously proposed by the authors [5] is summarized in Table 1, where  $\psi$  and  $\psi^0$  are the free energy per unit surface of the damaged and undamaged interface, respectively. The function  $\delta_{ij}$  is the Kronecker delta, and the variable  $d$  is a scalar damage variable. The parameter  $\lambda$  is the equivalent displacement jump norm. The equivalent displacement jump is a non-negative, continuous scalar function defined as:

$$\lambda = \sqrt{\langle \Delta_3 \rangle^2 + (\Delta_{shear})^2} \quad (5)$$

where  $\langle \cdot \rangle$  is the MacAuley bracket defined as  $\langle x \rangle = \frac{1}{2}(x + |x|)$ . The displacement jump in Mode I, i.e., normal to midplane is  $\Delta_3$ . The displacement jump tangent to the midplane,  $\Delta_{shear}$ , is the Euclidean norm of the displacement jump in Mode II and Mode III:

$$\Delta_{shear} = \sqrt{(\Delta_1)^2 + (\Delta_2)^2} \quad (6)$$

Table 1. Definition of the constitutive model.

Free Energy	$\psi(\Delta, d) = (1-d)\psi^0(\Delta_i) - d\psi^0(\delta_{3i}\langle -\Delta_3 \rangle)$
Constitutive equation	$\tau_i = \frac{\partial \psi}{\partial \Delta_i} = (1-d)\delta_{ij}K\Delta_j - d\delta_{ij}K\delta_{3j}\langle -\Delta_3 \rangle$
Displacement jump norm	$\lambda = \sqrt{\langle \Delta_3 \rangle^2 + (\Delta_{shear})^2}$
Damage criterion	$\bar{F}(\lambda^t, r^t) := G(\lambda^t) - G(r^t) \leq 0 \quad \forall t \geq 0$ $G(\lambda) = \frac{\Delta^f(\lambda - \Delta^o)}{\lambda(\Delta^f - \Delta^o)}$
Evolution law	$\dot{d} = \mu \frac{\partial \bar{F}(\lambda, r)}{\partial \lambda} = \mu \frac{\partial G(\lambda)}{\partial \lambda}$
Load/unload conditions	$\mu \geq 0$ ; $\bar{F}(\lambda^t, r^t) \leq 0$ ; $\mu \bar{F}(\lambda^t, r^t) = 0$ $r^t = \max\{\Delta^o, \max_s \lambda^s\} \quad 0 \leq s \leq t$

The evolution of damage is defined by a suitable monotonic scalar function,  $G(\cdot)$ , ranging from 0 to 1. A damage consistency parameter,  $\mu$ , is used to define loading-unloading conditions according to the Kuhn-Tucker relations.

Under crack closure during load reversal, the constitutive model prevents interpenetration of the faces of the crack by restoring the normal penalty stiffness of the element even in the presence of damage. Further details regarding the damage model can be found in references [4,5].

Under loading conditions, the damage variable is calculated as:

$$d = \frac{\Delta^f(\lambda - \Delta^o)}{\lambda(\Delta^f - \Delta^o)} \quad (7)$$

The relation between the damage variable  $d$ , representing the loss of stiffness, and the damage variable  $\bar{d}$ , representing the ratio of the energy dissipated over the fracture toughness the is given as [11]:

$$\bar{d} = \frac{A_d}{A^e} = \frac{\Xi}{G_c} = 1 - \frac{\lambda}{\Delta^o}(1-d) \quad (8)$$

Using Equations (7) and (8):

$$\frac{A_d}{A^e} = \frac{d\Delta^o}{\Delta^f(1-d) + d\Delta^o} \quad (9)$$

### 2.2.2 Constitutive model for high-cycle fatigue

Damage evolution that can be considered as the sum of the damage created by the quasi-static loads and the damage created by the cyclic loads:

$$\frac{dd}{dt} = \dot{d} = \dot{d}_{static} + \dot{d}_{cyclic} \quad (10)$$

The first term in the right hand side of Equation 10 is obtained from the equations

presented in previous section, while the second term needs to be defined to account for cyclic loading.

The evolution of the damage variable,  $d$ , is related with the surface crack growth rate,  $\frac{dA}{dN}$  as [11]:

$$\frac{\partial d}{\partial N} = \frac{\partial d}{\partial A_d} \frac{\partial A_d}{\partial N} \quad (11)$$

where  $A_d$  is the damaged area, and  $\frac{\partial A_d}{\partial N}$  is the growth rate of the damaged area. The term  $\frac{\partial d}{\partial A_d}$  can be obtained from (9):

$$\frac{\partial d}{\partial A_d} = \frac{1}{A^e} \frac{[\Delta^f (1-d) + d\Delta^o]^2}{\Delta^f \Delta^o} \quad (12)$$

#### Determination of the growth rate of the damaged area as a function of the number of cycles

Under cyclic loading, the damaged area grows as the number of cycles increase: after  $\Delta N$  cycles, the damaged area ahead of the crack tip increases by  $\Delta A_d$ . It is assumed that the increase in the crack area  $\Delta A$  is equal to the increase in the amount of damaged area. Therefore, the surface crack growth rate can be assumed to be equal to the sum of the damaged area growth rates of all damaged elements ahead of the crack tip:

$$\frac{\partial A}{\partial N} = \sum_{e \in A_{CZ}} \frac{\partial A_d^e}{\partial N} \quad (13)$$

where  $A_d^e$  is the damaged area of one element and the term  $A_{CZ}$  is the area of the cohesive zone. Taking  $\frac{\partial A_d}{\partial N}$  as the mean value of the damaged area growth rate  $\frac{\partial A_d^e}{\partial N}$  of the elements over the cohesive zone, and assuming that the mean area of the

elements in the cohesive zone is  $A^e$ , Equation 13 can be written as:

$$\frac{\partial A}{\partial N} = \sum_{e \in A_{CZ}} \frac{\partial A_d^e}{\partial N} = \frac{A_{CZ}}{A^e} \frac{\partial A_d}{\partial N} \quad (14)$$

where the ratio  $\frac{A_{CZ}}{A^e}$  represents the number of elements spanning the cohesive zone. Rearranging terms in Equation 14, the surface damage growth rate can be written as:

$$\frac{\partial A_d}{\partial N} = \frac{A^e}{A_{CZ}} \frac{\partial A}{\partial N} \quad (15)$$

#### Evolution of the damage variable under cyclic loading

Using Equations 12 and 15 in Equation 11 the evolution of the damage variable as a function of the number of cycles is given as:

$$\frac{\partial d}{\partial N} = \frac{1}{A_{CZ}} \frac{(\Delta^f (1-d) + d\Delta^o)^2}{\Delta^f \Delta^o} \frac{\partial A}{\partial N} \quad (16)$$

Under plane stress loading conditions, the area of the cohesive zone under mixed mode loading is given as:

$$A_{CZ} = b \frac{n+1}{\pi} \frac{E_{22}}{Q} \left[ (1-B) + B \sqrt{\frac{E_{11}}{E_{22}}} \right] \frac{G^{\max}}{(\tau^o)^2} \quad (17)$$

where  $G^{\max}$  is, for each integration point, the maximum energy release rate in the loading cycle,  $\tau^o$  is the interfacial strength,  $n$  is a material parameter that defines the tractions' distribution ahead of the crack tip [12],  $B$  is the mixed-mode ratio,

$$B = \frac{G_{II}}{G_I + G_{II}} \quad (18)$$

and  $Q$  is an elastic constant that reads:

$$Q = \frac{1}{2} \sqrt{2 \left[ \left( \frac{E_{22}}{E_{11}} \right)^{\frac{1}{2}} - \nu_{21} \right] + \frac{E_{22}}{G_{12}}} \quad (19)$$

The parameter  $b$  is the width of the delamination front. In the implementation in a Finite Element code, the parameter  $b$  is assumed to be equal to the characteristic length of the element.

### Crack growth rate

The surface crack growth rate under fatigue loading,  $\frac{\partial A}{\partial N}$ , is a load, geometric, and material-dependent characteristic that can be related to the Paris Law multiplying it with the crack front width:

$$\frac{\partial A}{\partial N} = b \frac{\partial a}{\partial N} \quad (20)$$

where  $\frac{\partial a}{\partial N}$  represents the growth rate. The typical pattern of the crack growth rate is shown in Figure 2.

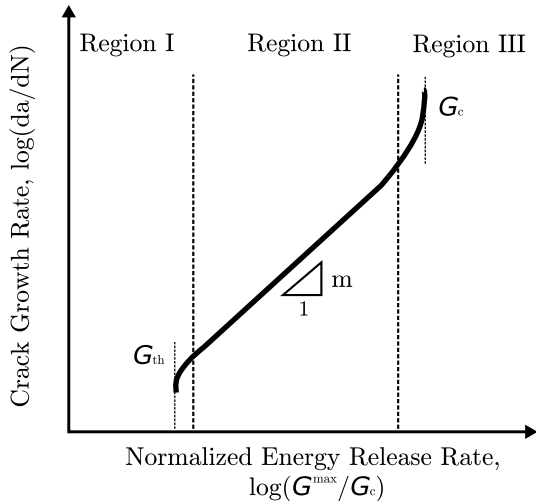


Figure 2. Typical crack growth rate regions.

In region I, crack growth is not observed if the maximum energy release rate is smaller than the fatigue threshold of the energy release rate,  $G_{th}$ . In

region III, the crack growth rate increases because the maximum energy release rate approaches the fracture toughness. Tearing fracture controls the crack growth rate in region III instead of fatigue propagation.

The crack growth rate  $\frac{\partial a}{\partial N}$  used in the fatigue damage model, Equation 20, is defined as a piecewise function defined as:

$$\frac{\partial a}{\partial N} = \begin{cases} C \left( \frac{\Delta G}{G_c} \right)^m, & G_{th} < G^{\max} < G_c \\ 0, & \text{otherwise} \end{cases} \quad (21)$$

where  $C$ ,  $m$  and  $G_c$  are parameters that depend on the mode-ratio.

Defining the load ratio,  $R$  as  $R^2 = \frac{G^{\min}}{G^{\max}}$ , the variation of the energy release rate is given as:

$$\Delta G = \frac{\tau^o}{2} \left[ \Delta^o + \frac{(\Delta^f - \lambda^{\max})^2}{\Delta^f - \Delta^o} \right] (1 - R^2) \quad (22)$$

The material parameters,  $C, m, G_{th}$  used in Equation 21 depend on the mode ratio. In Mode I loading, the crack growth rate parameters are  $C_I$ ,  $m_I$ , and  $G_{Ith}$ . For Mode II loading, the crack growth rate parameters are  $C_{II}$ ,  $m_{II}$ , and  $G_{IIth}$ . Under mixed-mode loading, the crack growth rate parameters  $C$ ,  $m$ , and  $G_{th}$  are given as [13]:

$$\log C = \log C_I + \left( \frac{G_{II}}{G_T} \right) \log C_m + \left( \frac{G_{II}}{G_T} \right)^2 \log \frac{C_{II}}{C_m C_I} \quad (23)$$

$$m = m_I + m_m \left( \frac{G_{II}}{G_T} \right) + (m_{II} - m_I - m_m) \left( \frac{G_{II}}{G_T} \right)^2 \quad (24)$$

where  $C_m$  and  $m_m$  are mode-ratio material parameters that must be determined by curve-fitting experimental data.

The dependence of the energy release rate threshold is given as [11]:

$$G_{th} = G_{Ith} + (G_{IIth} - G_{Ith}) \left( \frac{G_{shear}}{G_T} \right)^{\eta_2} \quad (25)$$

where  $\eta_2$  is a material parameter obtained from a curve-fit of experimental results.

### 2.2.3 Cycle jump strategy

For high-cycle fatigue, a cycle-by-cycle analysis becomes computationally intractable. Therefore, a cycle jump strategy needs to be implemented in the finite element model

The cycle jump strategy proposed computes the damage variable  $d_i^J$  at an integration point  $J$  after  $N_i$  cycles using the quasi-static constitutive equations. The predicted evolution of the damage variable with the number of cycles,  $\frac{\partial d}{\partial N}$ , is calculated using Equation 16. The damage variable at an integration point  $J$  after  $\Delta N_i$  cycles is:

$$d_{i+\Delta N_i}^J = d_i^J + \frac{\partial d_i^J}{\partial N} \Delta N_i \quad (26)$$

To determine the number of cycles  $\Delta N_i$  that can be skipped with a controlled level of accuracy, the following equation is used:

$$\Delta N_i = \frac{\Delta d_{max}}{\max_J \left\{ \frac{\partial d_i^J}{\partial N} \right\}} \quad (27)$$

where  $\Delta d_{max}$  is a small pre-established value.

## 3 Results

The present model is implemented as a user-written finite element in ABAQUS [6] by adding the fatigue damage model to the constitutive behavior of a cohesive element previously developed [4,5].

Simulations of Mode I, Mode II and Mixed-Mode delamination tests were conducted to demonstrate that when the constitutive damage model is used in a structural analysis, the analysis can reproduce the response of the test specimens without the use of any model-specific adjustment parameters.

The finite element model is composed of 4-node plane strain elements for the arms, which are connected by 4-node cohesive elements representing the interface. Two elements are used through the thickness, of each arm. The length of the element is 0.05mm. The details of the finite element model and the boundary conditions used in the simulations can be found in reference [11].

The material properties used in the simulations are obtained from references [14,15] and using Equations (23-25). The data introduced in the FEM are summarized in Tables 2 and 3.

Table 2. Static properties of HTA/637C carbon/epoxy laminates [14,15].

$E_{11}$ (GPa)	$E_{22}=E_{33}$ (GPa)	$G_{12}=G_{13}$ (GPa)	$G_{23}$ (GPa)
120	10.5	5.25	3.48
$\nu_{12}=\nu_{13}$	$\nu_{23}$	$\eta$	
0.30	0.51	1.45	
$G_{Ic}$ (kJ/m <sup>2</sup> )	$G_{IIc}$ (kJ/m <sup>2</sup> )	$\tau_{2=1}^o$ (MPa)	$\tau_3^o$ (MPa)
0.260	1.002	30	30

Table 3. Fatigue properties of HTA/637C carbon/epoxy laminates [14,15].

$C_I$ (mm/cycle)	$C_{II}$ (mm/cycle)	$C_m$ (mm/cycle)
0.0308	0.149	22904
$m_I$	$m_{II}$	$m_m$
5.4	4.5	4.94
$G_{Ith}$ (kJ/m <sup>2</sup> )	$G_{IIth}$ (kJ/m <sup>2</sup> )	$\eta_2$
0.060	0.100	2.73

### 3.1. Simulation of Mode I delamination test

The results obtained for the mode I simulation and the experimental data are shown in Figure 3. It can be observed that the constitutive model accounts for all three regions of fatigue crack growth. In region II, where crack growth rates follow the Paris Law, it is observed that a good agreement between the predictions and the experimental data is obtained. In region I there is negligible crack growth rate for small values of the normalized energy release rate and the numerical data follows the trend of the experimental data. A significant difference between the numerical and the experimental data is observed in region III. One of the reasons for this difference is that the crack growth rates present in region III are very high and, therefore, a low-cycle instead of a high-cycle fatigue model is more appropriate for this region. However, in spite of this difference, the model can also predict Region III crack growth rate, where the Paris Law equation is not valid.

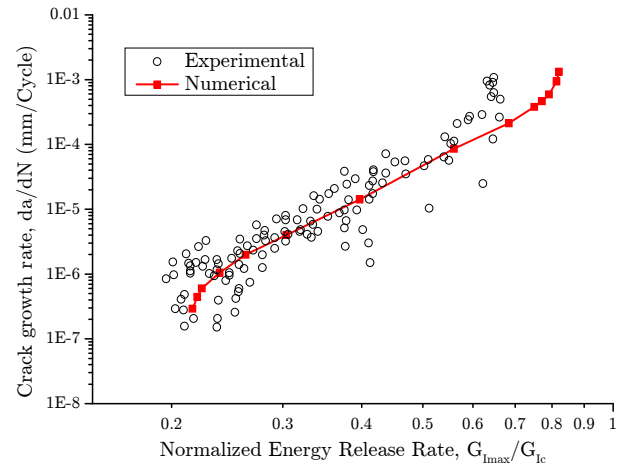


Fig. 3. Mode I crack growth rate.

The evolution of the crack tip position with the number of cycles for a normalized energy release rate of 40% is shown in Figure 4.

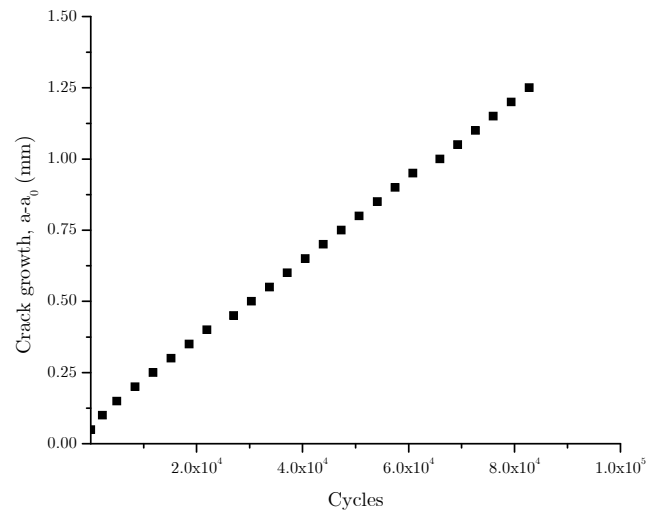


Fig. 4. Crack growth with the load cycles.

The model can be used to predict delamination onset. The number of cycles to decrease the global compliance of the DCB specimen for different levels of the maximum applied energy release rate is shown in Figure 5.

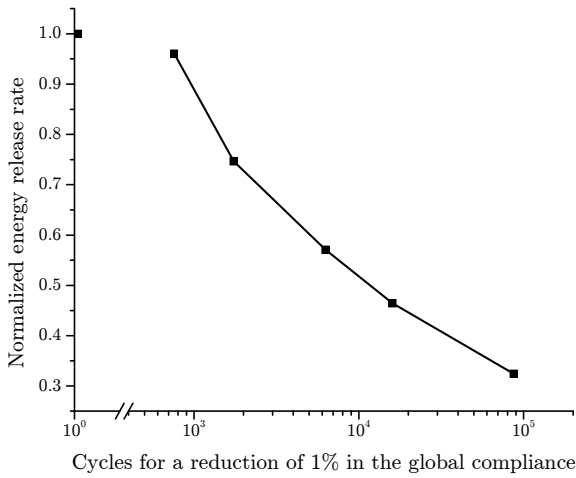


Fig. 5. Load cycles to a decrease of 1% the global compliance of the DCB test.

Several DCB tests were simulated to verify the sensitivity of the model to the load ratio. The results obtained from the simulations are shown in Figure 6 where it can be observed that higher load ratios decrease the crack growth rate.

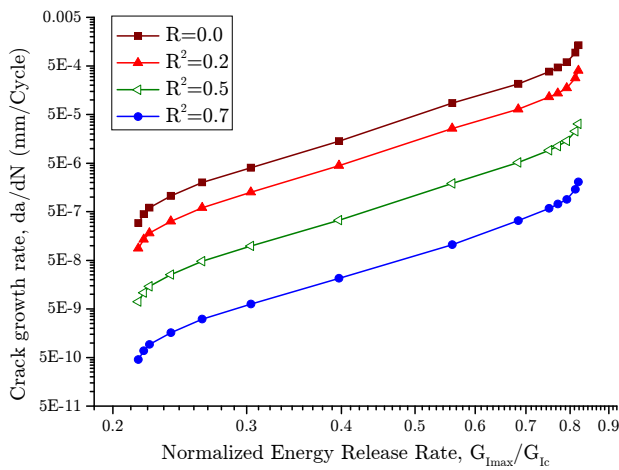


Fig. 6. Load ratio effect on the mode I crack growth rate.

The sensitivity of the constitutive model to the load ratio is an asset of the model. The sensitivity of the propagation rate to the load ratio derives directly from the quasi-static model rather than from a fatigue model defined as a function of the load ratio.

### 3.1. Simulation of Mode II delamination test

Several tests were conducted to simulate the crack growth rate under Mode II loading for different ranges of the energy release rate. Experimental data on fatigue driven delamination growth reported in [14,15] was selected for comparison.

For pure Mode II, the specimen was loaded using the four point End Notched Flexure (4ENF)

The finite element model used was similar to that used in the simulation of the Mode I.

The results obtained from the simulations and the experimental data [14] are shown in Figure 8. A good accuracy between the experimental and numerical data is observed. The numerical results are in a better agreement with the experimental data than those presented in [11]. The difference is on the better prediction of the length of the cohesive zone taking into account the orthotropy effects on the relation between the stress intensity factors and the energy release rate.

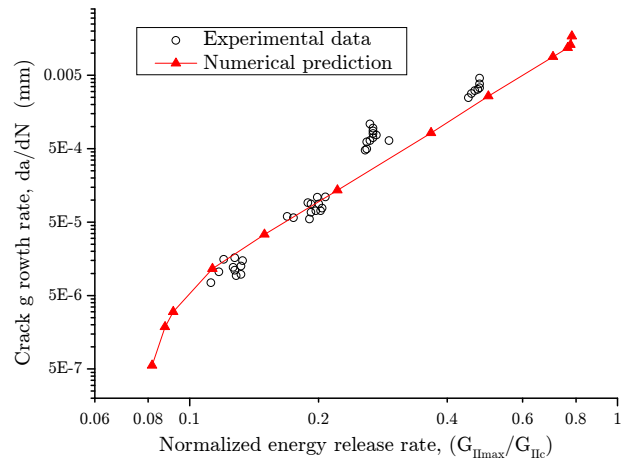


Fig. 8. Comparison of the experimental data with the crack growth rate obtained from the numerical simulation for a Mode II 4ENF test.

### 3.3. Simulation of mixed-mode loading

Several tests were conducted to simulate the crack growth rate under mixed-mode loading with for different energy release rates. Experimental data on fatigue driven delamination growth reported in [14] was selected for comparison. The dimensions and the material of the specimen are the same used for the DCB specimen described above.

The finite element model used was similar to that used in the simulation of the Mode I test.

The results obtained from the simulations and the experimental data [14] are shown in Figure 9. As in the pure mode tests, a good accuracy between the experimental and the predicted numerical data is observed.

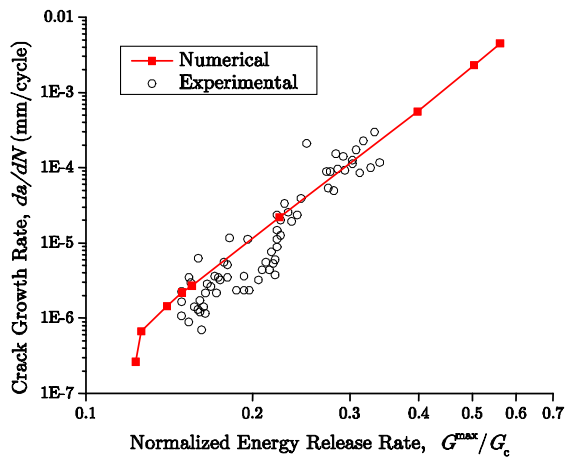


Fig. 9. Comparison of the experimental data with the crack growth rate obtained from the numerical simulation for a mixed-mode test.

### 3 Conclusions

A damage model suitable for both quasi-static and high-cycle fatigue delamination propagation was developed. The evolution of the damage variable was derived by linking Damage Mechanics and Fracture Mechanics, thus establishing a relation between damage evolution and crack growth rates. The damage evolution laws for cyclic fatigue were combined with the law of damage evolution for quasi-static loads within a cohesive element previously developed by the authors.

Simulations over specimens under Mode I, Mode II and mixed-mode loading were carried out. It is observed that the obtained results reproduce the three regions of the typical fatigue crack growth. In region II, where crack growth rates follow the Paris Law, it is observed that a good agreement between the predictions and the experimental data is obtained. In region I there is negligible crack growth rate for small values of the normalized energy release rate and the numerical data follows the trend of the experimental data. A significant difference between the numerical and the experimental data is observed in region III. One of the reasons for this difference is that the crack growth rates present in region III are very high and, therefore, a low-cycle instead of a high-cycle fatigue model is more appropriate for this region. However, in spite of this difference, the model can also predict region III crack growth rate, where the Paris Law equation is not valid.

Moreover, the results obtained from the simulations with different load ratio show that the model is sensitive to the load ratio. The higher load ratios the lower crack growth rate.

The model can be used to predict fatigue delamination onset, predicting the number of cycles to get a certain reduction of the global compliance of the specimen. The  $G^{max}$ - $N$  curve for a decrease of 1% the global compliance has been obtained from the Mode I simulations.

In summary, the model was able to reproduce the Paris Law growth rate without the need of any additional adjustment parameters. Moreover, the model accounts for the energy release rate thresholds preventing crack growth for smaller values of the energy release rate. Unlike other approaches proposed in the literature, where the dependence on the load ratio,  $R$ , is introduced through the definition of  $R$ -dependent Paris Law parameters, the effects of the load ratio on the analysis results is inherent to the formulation. The model is able to predict the crack growth rates in all regimes of propagation and the results compare favorably with the experimental data, including the negligible crack growth rates for small values of the normalized energy release rate and the sensitivity to the mode and load ratio.

## References

- [1] R. Peerling, W. Bredelmanns, R. de Borst, M. Geers, Gradient-enhanced damage modelling of high-cyclic fatigue, *International Journal of Numerical Methods in Engineering*, 9 (2000), 1547–1569.
- [2] P. Robinson, U. Galvanetto, D. Tumino, G. Bellucci, Numerical simulation of fatigue-driven delamination using interface elements, *International Journal of Numerical Methods in Engineering*, 63 (2005), 1824–1848.
- [3] J.J. Muñoz, U. Galvanetto and P. Robinson, On the numerical simulation of fatigue-driven delamination using interface elements, *International Journal of Fatigue*, 28(2006) 1136-1146.
- [4] P.P. Camanho, C.G. Dávila, M.F. de Moura, Numerical simulation of mixed-mode progressive delamination in composite materials, *Journal of Composite Materials*, 37(2003), 1415-1438,.
- [5] A. Turon, P.P. Camanho, J. Costa, C.G. Dávila, A damage model for the simulation of delamination in advanced composites under variable-mode loading, *Mechanics of Materials*, 38 (2006), 1079–1089.
- [6] Hibbit, Karlsson, Sorensen, ABAQUS 6.5 Users' Manuals, Pawtucket, USA, (2005).
- [7] Dugdale, D.S. Yielding of steel sheets containing slits. *Journal of Mechanics and Physics of Solids*, 8 (1960),100-104.
- [8] Barenblatt, G.I. The mathematical theory of equilibrium cracks in brittle fracture. *Advances in Applied Mechanics*, 7 (1962), 5-129.
- [9] A. Hillerborg, M. Modéer, P. Petersson, Analysis of crack formation and crack growth in concrete by means of fracture mechanics and finite elements, *Cement and Concrete Research*, 6 (1976), 773--782.
- [10] M. Ortiz, A. Pandolfi, Finite-deformation irreversible cohesive elements for three-dimensional crack propagation analysis, *International Journal for Numerical Methods in Engineering*, 44 (1999), 1267-82.
- [11] A. Turon, J. Costa, P.P. Camanho, C.G.Dávila, Simulation of delamination propagation under fatigue loading using cohesive zone models, *Composites Part A*, in Press, (2007).
- [12] Z.P. Bazant, J. Planas, *Fracture and size effect in concrete and other quasibrittle materials*, CRC Press, 1998.
- [13] N. Blanco, E.K. Gamstedt, L.E. Asp, J.Costa, Mixed-mode delamination growth in carbon-fibre composite laminates under cyclic loading, *International Journal of Solids and Structures* 41 (2004), 4219-4235.
- [14] L. Asp, A. Sjögren, E. Greenhalgh, Delamination growth and thresholds in a carbon/epoxy composite under fatigue loading, *Journal of Composites Technology and Research*, 23 (2001), 55-68.
- [15] M. Juntti, L. Asp, R. Olsson, Assessment of evaluation methods for the mixed-mode bending test, *Journal of Composites Technology and Research*, 21 (1999), 37-48.